JACS
JOURNAL OF THE AMERICAN CHEMICAL SOCIETY
Article
pubs.acs.org/JACS

Stabilization of Cucurbituril/Guest Assemblies via Long-Range Coulombic and CH···O Interactions

Roymon Joseph,[†] Anna Nkrumah,[†] Ronald J. Clark,[‡] and Eric Masson*[,†]

[†]Department of Chemistry and Biochemistry, Ohio University, Athens, Ohio 45701, United States
[‡]Department of Chemistry and Biochemistry, Florida State University, Tallahassee, Florida 32306, United States

Supporting Information

ABSTRACT: Cucurbit[*n*]urils (CB[*n*], *n* = 6−8) interact strongly with metal-bound 4′-substituted terpyridine ligands (M = Fe(II) and Ir(III)) via CH···O hydrogen bonding, despite significant separation between the positive metallic cation and the carbonylated rim of CB[*n*], and the location of the latter in the second coordination sphere of the metal ion. While water has been shown to mediate interactions between cations and CB[*n*]s in some assemblies, mediation by organic ligands is unprecedented. The recognition process is driven by the contrasted combination of extremely favorable binding enthalpies (up to 20.2 kcal/mol) and very unfavorable entropic components (as low as −10.2 kcal/mol). Dynamic oligomers were prepared in the presence of CB[8], which acts as a "soft", noncovalent linker between metal/terpyridine complexes, and interconnects two 4′-substituents inside its cavity. Social self-sorting between CB[8] and metal/terpyridine complexes bearing 4′-(2-naphthyl) and 4′-(2,3,5,6-tetrafluorophenyl) substituents was also observed, and could afford well-organized oligomers with alternating Fe(II) and Ir(III) cations.

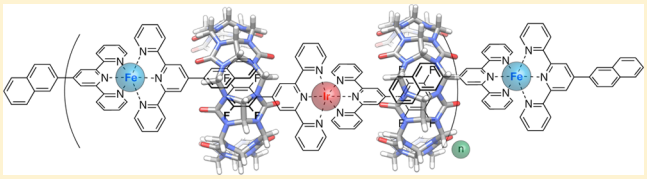

INTRODUCTION

Some three decades ago, Mock and co-workers showed that Cucurbit[6]uril (CB[6])[1] formed tight complexes with positively charged amphiphilic guests. Complex formation was attributed to the interaction between the positive charges and the carbonylated portals of CB[6], and between the hydrophobic moiety of the guests and the hydrophobic cavity of the macrocycle. While this assessment remains generally valid, the pioneering work by Kaifer, Isaacs, Gilson, Kim and Inoue,[2] as well as Nau and co-workers[3] afforded a much more detailed and subtle description of the recognition process. Briefly, the extreme binding affinities often observed with CB[*n*]s are caused by (1) the ability of the guests, in particular positively charged ones, to return as many hydration water molecules as possible to the bulk upon binding (a process that is both enthalpically and entropically favorable); (2) as mentioned above, favorable ion-dipole interactions between positively charged substituents and the CB[*n*] rims, and other Coulombic contributions such as hydrogen bonding; however, the magnitude of the interaction is severely hampered by a loss of solvation upon encapsulation; (3) the rigidity of the macrocycles and the limited degrees of rotational freedom of some guests (an entropic advantage); and (4) van der Waals interactions between the inner wall of CB[*n*]s and the surface of the guests; the magnitude of this contribution is a subject of controversy: while attractive dispersive interactions reach a maximum when the separation between two atoms is approximately 3 Å[4] (a distance that is likely to be present between several pairs of host and guest atoms), Nau showed that the cavity of CB[7] is overall highly unpolarizable.[3]

Coulombic interactions between positive units and the portals of CB[*n*]s can be caused by direct contact between a metallic or organic cation and the carbonyl laced portal of the macrocycle,[5] or by water mediation between the two units as it is often the case with transition metals and clusters in the solid state.[5d,6] Here, we report for the first time that Coulombic interactions between a metal and CB[*n*]s can be mediated by an organic ligand, and we show that even in the second coordination sphere, CB[*n*]s form remarkably strong CH···O hydrogen bonds with the ligand surrounding the metallic core.

RESULTS AND DISCUSSION

A set of terpyridine ligands **1**−**3**, bearing 4-tolyl, 2-naphthyl, and 2,3,5,6-tetrafluorophenyl substituents at position 4′, respectively, were prepared, followed by their complexes with Fe(II) and Ir(III) cations (chloride and nitrate as their counteranions, respectively; see Scheme in Figure 1).[7] The interaction of the six metal/ligand complexes with CB[7] was then monitored by ^{1}H nuclear magnetic resonance spectroscopy (NMR). The 4-tolyl group of complexes $[Fe{\cdot}\mathbf{1}_2]^{2+}$ and $[Ir{\cdot}\mathbf{1}_2]^{3+}$ was found to sit inside the cavity of the macrocycle, with strong upfield shifts of hydrogen nuclei located at positions 2 and 3 of the 4-tolyl unit (up to 1.04 ppm; noted 7 and 8 in Figure 1), and of the methyl hydrogens at its 4-position (up to 0.52 ppm) being measured upon complexation. The encapsulation of the 2-naphthyl and 2,3,5,6-tetrafluorophenyl groups in complexes $[Fe{\cdot}\mathbf{2}_2]^{2+}$, $[Fe{\cdot}\mathbf{3}_2]^{2+}$, $[Ir{\cdot}\mathbf{2}_2]^{3+}$, and $[Ir{\cdot}\mathbf{3}_2]^{3+}$ was also confirmed by upfield shifts of the relevant units. As

Received: September 12, 2013
Published: April 16, 2014

   dx.doi.org/10.1021/ja4092165 | *J. Am. Chem. Soc.* 2014, 136, 6602−6607

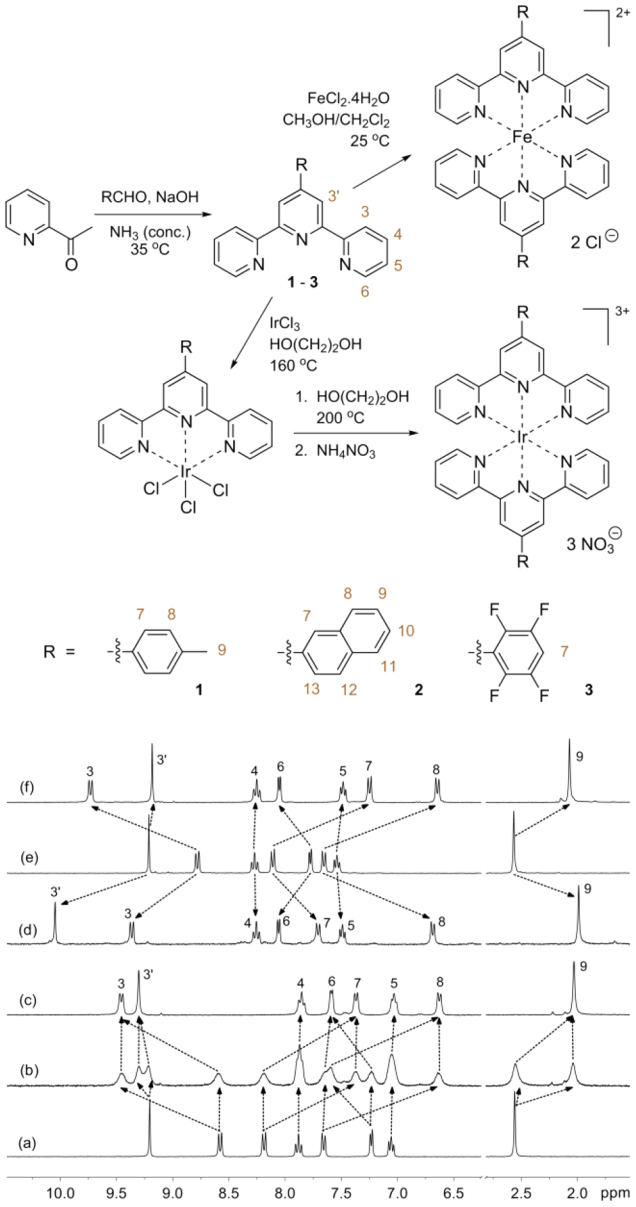

Figure 1. Preparation of metal–ligand complexes. ^{1}H NMR spectra of complex $[Fe{\cdot}\mathbf{1}_2]^{2+}$ (a) in the absence of CB[7], and after addition of (b) 1.0 equiv and (c) 2.0 equiv of CB[7]; ^{1}H NMR spectra of (d) assembly $[Ir{\cdot}\mathbf{1}_2]^{3+}{\cdot}(CB[6])_2$, (e) free metal–ligand complex $[Ir{\cdot}\mathbf{1}_2]^{3+}$, and (f) its inclusion complex with two CB[7] macrocycles.

expected, saturation was reached upon addition of 2.0 equiv of CB[7], until the terpyridine 4′-substituents were fully encapsulated. Unexpectedly, exchanges between the metal–ligand complexes and CB[7] were slow on the NMR time scale (see Figure 1, spectrum b); this is in stark contrast with the *p*-tolylmethylammonium cation (**4**) which undergoes a faster intermediate exchange with CB[7], despite a direct contact between the positive ammonium group and the carbonylated rim of CB[7]. Also, exceptionally strong downfield shifts of hydrogens located at positions 3 and 3″ of the terpyridine ligands (between 0.65 and 1.12 ppm among the 6 complexes), and significant downfield shifts of the opposite 6 and 6″-hydrogens (0.26 to 0.37 ppm) were measured. These singularities led us to consider possible CH···O hydrogen bonds between these hydrogen atoms and the oxygens of the carbonylated portals of CB[7]; unusually strong downfield shifts of the CH donor hydrogens are indeed symptomatic of such interactions.[8] Chemical shifts observed upon interaction of complex $[Ir{\cdot}\mathbf{1}_2]^{3+}$ with CB[6] are also consistent with this statement. A 0.82 ppm downfield shift was observed for H(3′) hydrogens this time (see Figure 1, spectrum d), while H(3) and H(3″) nuclei underwent weaker shifts than when sitting at the portal of CB[7] (0.57 vs 0.95 ppm). Hydrogen bonds between H(3′) atoms and the closest CB[6] oxygens are consistent with a shorter and tighter penetration of the tolyl head of the metal–ligand complex into CB[6] due to the reduced diameter of the latter.

No CB[*n*]-containing assembly afforded crystals suitable for quality X-ray diffraction. To circumvent this problem, we carried out two-dimensional nuclear Overhauser effect spectroscopy (NOESY) experiments using assembly $[Ir{\cdot}\mathbf{1}_2]^{3+}{\cdot}(CB[7])_2$. This technique has been used on several occasions to quantify through-space distances in solution, by gradually increasing mixing times and monitoring the growth of the cross peaks attributed to the interactions between hydrogen nuclei.[9] In this case, we monitored the interaction of hydrogens at position 3 and 3″ of the terpyridine ligands with the methylene hydrogens of CB[7] that point toward the metallic core. Also in parallel, we optimized the structure of assembly $[Ir{\cdot}\mathbf{1}_2]^{3+}{\cdot}(CB[7])_2$ at the TPSS-D3(BJ)/def2-SVP level[4a,10] with the COSMO solvation model[11] (see Figure 2; our choice of

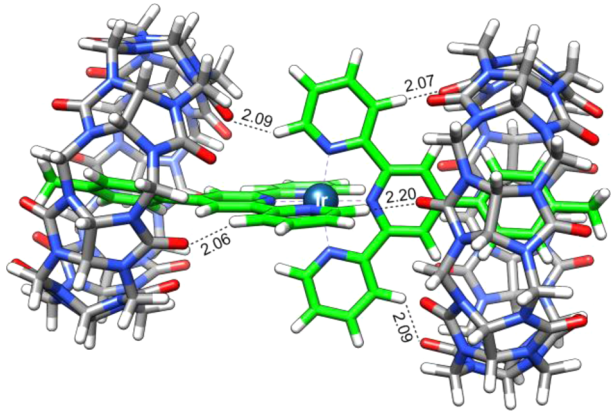

Figure 2. Optimized structure of complex $[Ir{\cdot}\mathbf{1}_2]^{3+}{\cdot}(CB[7])_2$, calculated at the TPSS-D3(BJ)/def2-SVP level with the COSMO solvation model. Distances between host and guest atoms are given in angstroms (Å).

functional was based on its high accuracy in the treatment of both transition metal complexes[12] and supramolecular systems).[4b] The r^{-6}-weighted average distance (see Supporting Information for details) between H(3) or H(3″) atoms and the hydrogens at the CB[7] portal was found to be 3.92 (±0.02) Å when determined by NOESY experiments and 3.87 Å in the calculated structure. Consequently, the excellent agreement between both methods allowed us to use the structure obtained in silico to evaluate distances between H(3) atoms and the nearest CB[7] oxygens, as well as C(3)–H(3)–O angles. Distances were 2.08 (±0.02) Å and CHO angles 132–161°, well within the range deemed acceptable for hydrogen bonding (distances shorter than 2.5 Å and angles narrower than 110°).[13]

The binding affinities of the metal–ligand complexes toward CB[7] were then determined by isothermal titration calorimetry (ITC). They not only surprised us by their magnitude (ranging from 3.4×10^6 to 3.8×10^7 M^{-1}, see Supporting

dx.doi.org/10.1021/ja4092165 | J. Am. Chem. Soc. 2014, 136, 6602–6607

Information for details), but also by their lack of dependence on the nature of the metal, and their very unfavorable entropic component (as low as −10.2 kcal/mol at 25 °C, the lowest parameter ever measured with CB[7], see Figure 3). As a

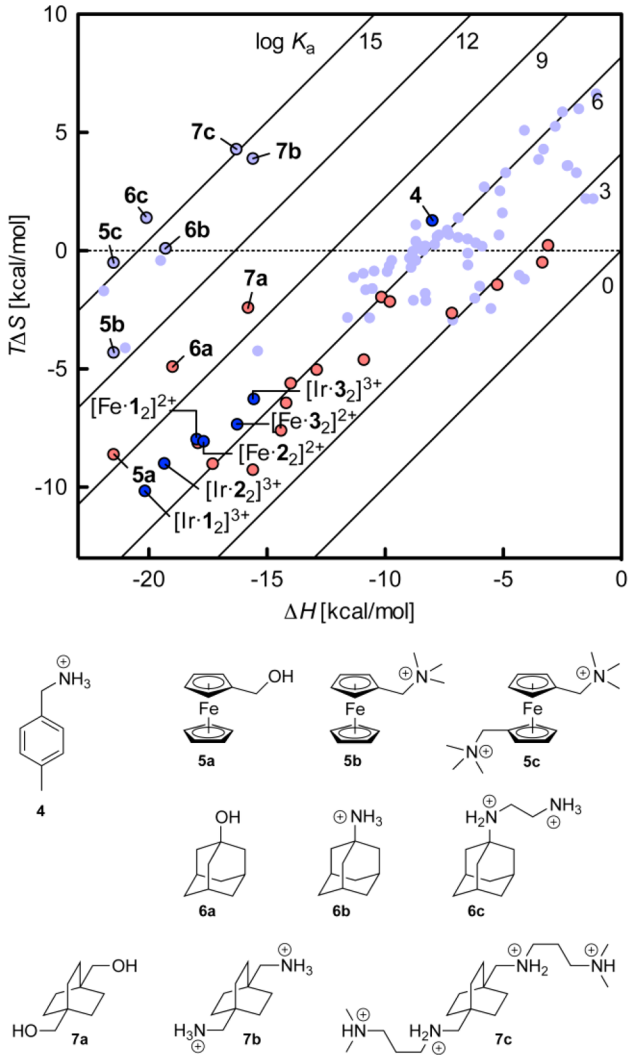

Figure 3. Enthalpy−entropy compensation plot for the interaction of CB[7] with various guests,[3b,16] including the metal−ligand complexes described in this study. Light blue and pink dots represent positive and neutral[3b,16a−c] guests, respectively.

reference, we also determined the binding affinity of CB[7] toward the *p*-tolylmethylammonium cation (**4**; 6.4 × 10^6 M^{-1}). Although its binding affinity is similar to the metal−ligand complexes, its binding entropy is much more favorable (+1.3 kcal/mol at 25 °C), but is compensated by a weaker enthalpic contribution (see Figure 3). Titrations were suitably fitted with a 1:1 binding model, thereby indicating that the presence of one CB[7] unit on the metal−ligand complex does not significantly affect the affinity of the second opposite macrocycle. This observation is in stark contrast with the behavior of disubstituted ammonium cations, which can accommodate only one CB unit per ammonium group.[1c,14]

To rationalize these thermodynamic parameters, one needs to reexamine the landmark studies by Kaifer, Isaacs, Gilson, Kim, Inoue and co-workers,[2] related to the CB[7] encapsulation of ferrocene, adamantane and bicyclo[2.2.2]octane derivatives bearing neutral and positively charged substituents (see Figure 3, guests **5**−**7**). These authors showed that the gain in binding affinities when positively charged groups interact with the rim of CB[7] is solely an entropic effect, at least in these cases. Since the solvation of positive species is more entropically penalizing compared to neutral structures,[15] their partial desolvation upon CB[7] binding (i.e., the return of water molecules to the bulk) must therefore be more entropically favorable. As shown in Figure 3 (see pink dots), an overview of published thermodynamic parameters reveals that all neutral guests with significant affinities toward CB[7] (>10^3 M^{-1}) suffer from an entropic impediment upon binding. The constant binding enthalpies along the series of guests **5**−**7** are likely caused by a perfect balance between host−guest electrostatic interactions (which increase dramatically when positive charges are present) and unfavorable enthalpies of desolvation upon binding, that follow the same trend.[2]

For those same reasons, the binding entropy measured with guest **4** is positive, since CB[7] becomes part of the first coordination sphere, and returns constrained water molecules to the bulk. In the case of our metal−ligand complexes, CB[7] is located in the *second* coordination sphere upon binding, and replaces water molecules whose arrangement around the charged complex is much less ordered, hence a marked decrease in binding entropy. We attribute the more favorable enthalpic component of the interaction, compared to guest **4**, to the three strongly positive points of contact presented to CB[7] (H(3), H(3″) on the terpyridine ligand, as well as one H(6) atom of its opposite neighbor; see Figure 2). Figure 4a

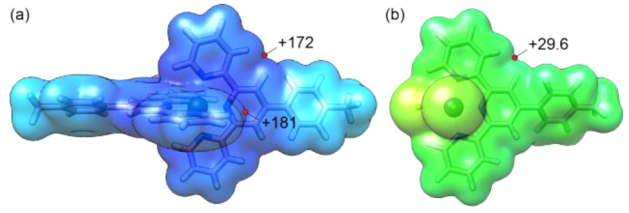

Figure 4. Electrostatic potential maps of complexes (a) $[Ir{\cdot}\mathbf{1}_2]^{3+}$ and (b) $IrCl_3{\cdot}\mathbf{1}$, superimposed on the isodensity surface of the structures (isovalue 0.002) and probed with a positive point charge. Calculations carried out at the TPSS-D3(BJ)/def2-SVP level; energies in kilocalorie per mole (kcal/mol). Color-coding: dark blue, light blue, green, yellow, and red correspond to +200, +100, 0, −100, and −200 kcal/mol, respectively.

shows an electrostatic potential map of guest $[Ir{\cdot}\mathbf{1}_2]^{3+}$; the most electropositive regions of the potential surface are located at the top of both pairs of H(3) and H(6) atoms (+172 and +181 kcal/mol, respectively; as a reference, the electrostatic potential surrounding the hydrogens of the ammonium cation in guest **4** reaches +165 kcal/mol).

To stress the importance of the radiating positive charge emanating from the metallic cation, we compared the binding affinities of CB[7] toward complex $[Ir{\cdot}\mathbf{1}_2]^{3+}$ and its analogue $IrCl_3{\cdot}\mathbf{1}$, that bears only one terpyridine ligand; the comparison was carried out in dimethyl sulfoxide-d^6 (DMSO) since complex $IrCl_3{\cdot}\mathbf{1}$ is insoluble in aqueous medium. The binding affinity of complex $[Ir{\cdot}\mathbf{1}_2]^{3+}$ still reached 3.7 × 10^2 M^{-1}, despite DMSO being a much better hydrogen bond acceptor than water (and as a result, a better candidate than water when competing for solute interactions against CB[7]);[17] the ejection of aprotic DMSO from the cavity of CB[7] to the bulk upon

dx.doi.org/10.1021/ja4092165 | J. Am. Chem. Soc. 2014, 136, 6602−6607

binding is also likely less favorable than the ejection of water (water−water interactions are less than optimal inside CB[7], hence the energetically favorable ejection). In complex $IrCl_3$·**1**, however, the partially negative chlorine ligands dramatically decrease the positive potential at the surface of H(3) and H(3″) (from +172 to +29.6 kcal/mol, see Figure 4b), resulting in a complete loss of affinity toward CB[7]. These results suggest that C−H···O hydrogen bonding between the metal−ligand complex and the carbonylated rims of CB[*n*]s is only enabled in the presence of a neighboring positive charge. The ligand can then be seen as an area of low relative permittivity that allows the propagation of the charge toward the periphery of the complex and the CB[*n*] portals. We also attribute the favorable binding enthalpy of our metal−ligand complexes to a less penalizing enthalpy of desolvation upon CB[7] binding, due to the longer separation between second coordination sphere water molecules and the metallic cation; a similar effect has been observed when comparing the solvation enthalpies of ammonium and tetramethylammonium cations (−78 vs −51 kcal/mol, respectively).[15]

The recognition properties of the metal−ligand complexes were extended to CB[8] (4′-substituents in terpyridines **2** and **3** were specifically chosen to interact with this macrocycle). As shown by Zhang and co-workers,[18] CB[8] can encapsulate two naphthyl units into its cavity when they are flanked by positively charged groups. In our case, Coulombic and CH···O hydrogen bonding on both portals of CB[8] led to the formation of a dynamic supramolecular oligomer in the presence of stoichiometric amounts of CB[8] and complexes $[Fe{\cdot}\mathbf{2}_2]^{2+}$ and $[Ir{\cdot}\mathbf{2}_2]^{3+}$ (see Figure 5). This is supported by the

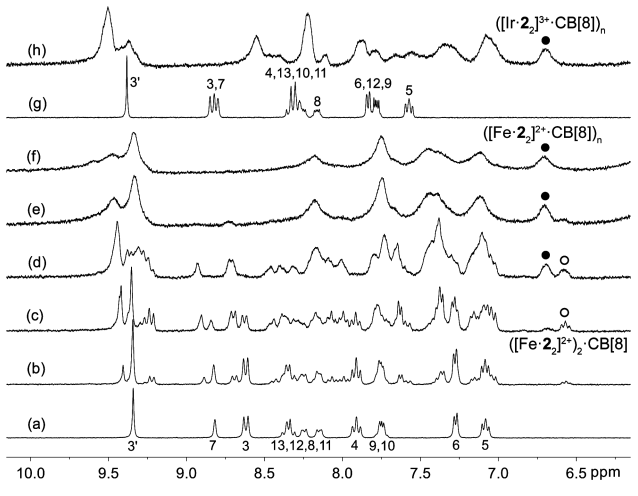

Figure 5. ^{1}H NMR spectra of complex $[Fe{\cdot}\mathbf{2}_2]^{2+}$ (2.0 mM) (a) in the absence of CB[8], and (b−f) with increasing amounts of CB[8] (up to 2.0 mM). ^{1}H NMR spectra of complex $[Ir{\cdot}\mathbf{2}_2]^{3+}$ (g) in the absence of CB[8], and (h) in the presence of a stoichiometric amount of the macrocycle. Black circles and dots highlight the signature signals of the two modes of naphthyl/naphthyl interaction inside CB[8].

very strong upfield shifts of the naphthyl hydrogen nuclei upon interaction with CB[8] (approximately 1.1 ppm, see Figure 5, spectra a−f), as well as the observed signal broadening indicating an increase in correlation time, shorter transverse relaxation times and hence a large increase in the molecular weight of the assemblies. In addition, the aromatic region of the ^{1}H NMR spectra is not altered in the presence of an excess amount of CB[8], thereby indicating that the latter is present as free CB[8] above 1.0 equiv. Diffusion-ordered NMR spectroscopy experiments (DOSY) yielded diffusion coefficients D = 2.8×10^{-10} and 7.1×10^{-11} m^2/s for complex $[Fe{\cdot}\mathbf{2}_2]^{2+}$ and its CB[8]-containing oligomer, respectively, at a 2.0 mM concentration. The molecular weight (M) dependence on the diffusion coefficients follows the power law $D \propto M^{-m}$, where m ranges from approximately 0.3 to 0.6 depending on the nature of the polymer.[19] After calibration with assemblies of known molecular weights and diffusion coefficients (see Supporting Information section), we extracted an approximate value for m (0.47).

The approximate average molecular weight of oligomer $([Fe{\cdot}\mathbf{2}_2]^{2+}{\cdot}CB[8])_n$ is thus 2.4×10^4 g/mol, which corresponds to 11 monomers held together by CB[8]. A heavier average molecular weight (1.2×10^5 g/mol, corresponding to 54 monomeric units) was found in the case of oligomer $([Ir{\cdot}\mathbf{2}_2]^{3+}{\cdot}CB[8])_n$ at a 1.0 mM concentration. We do stress, however, that molecular weights extrapolated from DOSY experiments suffer from significant uncertainty, which may reach factors of approximately 3 at 10^5 g/mol.

We note a peculiar feature of the ^{1}H NMR spectrum of iron and iridium complexes of ligands **2** and **3** in the presence of increasing, yet substoichiometric amounts of CB[8] (see the case of complex $[Fe{\cdot}\mathbf{2}_2]^{2+}$ in Figure 5): a symmetrical multiplet belonging to the CB[8]-encapsulated 2-naphthyl substituent first appears at 6.57 ppm (see black circles in Figure 5), and upon further addition of the macrocycle, dissipates as another naphthyl signal of oligomer $([Fe{\cdot}\mathbf{2}_2]^{2+}{\cdot}CB[8])_n$ forms (6.70 ppm; black dots). DOSY experiments yielded a diffusion coefficient of 1.7×10^{-10} m^2/s and a 2.8×10^3 g/mol molecular weight for the assembly at low CB[8] concentration; therefore, we assign its structure as $([Fe{\cdot}\mathbf{2}_2]^{2+})_2{\cdot}CB[8]$ (M = 2877 g/mol). The existence of two sets of discrete signals for this short dimer and the longer oligomers indicates a slightly different organization of the pair of naphthyl units inside CB[8] in these two cases. We suggest that the connection of an additional $[Fe{\cdot}\mathbf{2}_2]^{2+}{\cdot}CB[8]$ fragment to the short dimer $([Fe{\cdot}\mathbf{2}_2]^{2+})_2{\cdot}CB[8]$ benefits from positive cooperativity originating from the iron cation located two metals away: electrostatic potential maps indicate that the positive surface area of dimer $([Fe{\cdot}\mathbf{2}_2]^{2+})_2{\cdot}CB[8]$ available for subsequent $[Fe{\cdot}\mathbf{2}_2]^{2+}{\cdot}CB[8]$ binding is significantly more electropositive (+155 and +152 kcal/mol above position H(3) and H(6), respectively, see Figure 6a) than the same area in free metal−ligand complex $[Fe{\cdot}\mathbf{2}_2]^{2+}$ (+134 and +133 kcal/mol above H(3) and H(6), see Figure 6b).

CB[8] also encapsulates two 2,3,5,6-tetrafluorophenyl units, and dynamic oligomers of complexes $[Fe{\cdot}\mathbf{3}_2]^{2+}$ and $[Ir{\cdot}\mathbf{3}_2]^{3+}$ are formed with a stoichiometric amount of the macrocycle (see Figure 7; M = 5.8×10^4 and 3.5×10^4 g/mol, corresponding to 27 and 15 monomeric units, respectively, at 2.0 mM). However, the appearance of a new signal at 7.1 ppm in the presence of excess CB[8] (see crossed circles in spectra c and f) suggests that binary complexes between CB[8] and the tetrafluorophenyl units (affording assemblies $[M{\cdot}\mathbf{3}_2]^{n+}{\cdot}(CB[8])_2$), compete with the ternary complexes responsible for the formation of the oligomers (black dots).

Finally, we tested whether CB[8] would opt for narcissistic or social self-sorting in the presence of equimolar amounts of homo-oligomers $([Fe{\cdot}\mathbf{2}_2]^{2+}{\cdot}CB[8])_n$ and $([Ir{\cdot}\mathbf{3}_2]^{3+}{\cdot}CB[8])_n$. The disappearance of the signature signal for the encapsulated naphthyl dimer at 6.70 ppm (see Figure 8, spectra a and c, black dots and the fact that iridium−terpyridine complexes were

dx.doi.org/10.1021/ja4092165 | J. Am. Chem. Soc. 2014, 136, 6602−6607

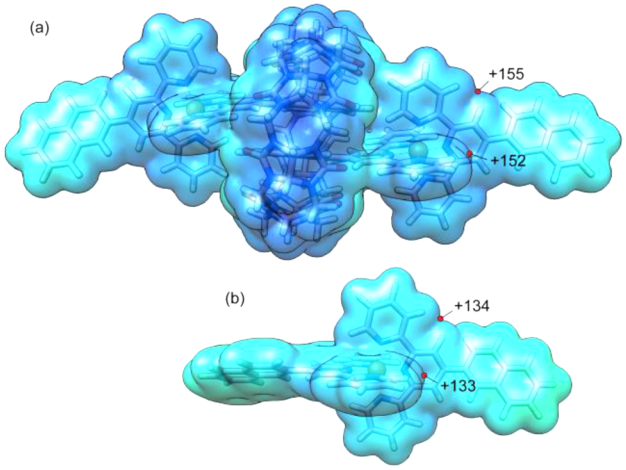

Figure 6. Electrostatic potential maps of complexes (a) $([Fe{\cdot}\mathbf{2}_2]^{2+})_2{\cdot}CB[8]$ and (b) $[Fe{\cdot}\mathbf{2}_2]^{2+}$, superimposed on the isodensity surface of the structures and probed with a positive point charge. See Figure 4 for calculation method and color-coding.

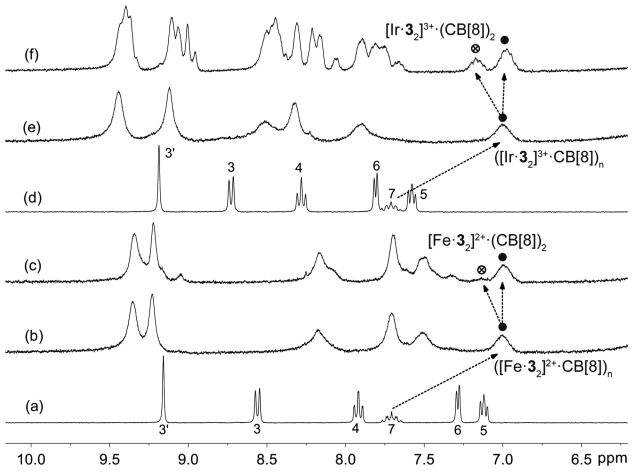

Figure 7. ^{1}H NMR spectra of complex $[Fe{\cdot}\mathbf{3}_2]^{2+}$ (a) in the absence of CB[8], and in the presence of (b) a stoichiometric amount of CB[8], and (c) 2.5 equiv of CB[8]. Spectra (d–f) were obtained similarly with complex $[Ir{\cdot}\mathbf{3}_2]^{3+}$.

found not to be labile indicate by transposition the quantitative formation of the alternating "social" hetero-oligomer $([Fe{\cdot}\mathbf{2}_2]^{2+}{\cdot}CB[8]{\cdot}[Ir{\cdot}\mathbf{3}_2]^{3+}{\cdot}CB[8])_n$![20]

Signature signals of the latter are highlighted with black squares in Figure 8. The clear preference for naphthyl/tetrafluorophenyl encapsulation inside CB[8] to the expense of the corresponding homodimers is likely due to favorable quadrupole–quadrupole interactions in the former case (this is reminiscent of the iconic interaction between benzene and perfluorobenzene).[21] Similar observations were made upon combination of assemblies $([Ir{\cdot}\mathbf{2}_2]^{3+}{\cdot}CB[8])_n$ and $([Fe{\cdot}\mathbf{3}_2]^{2+}{\cdot}CB[8])_n$ (see Figure 8, spectra d–f).

In conclusion, we have shown that (1) CB[n] macrocycles can form tight complexes with guests bearing a positive core, even when the former occupy the second coordination sphere; (2) like water in the solid state, organic ligands such as functionalized terpyridines can act as mediators between the positive charge and the carbonylated portal of CB[n]s, resulting in the formation of favorable CH···O interactions; and (3) well-organized dynamic oligomers can be formed in the presence of

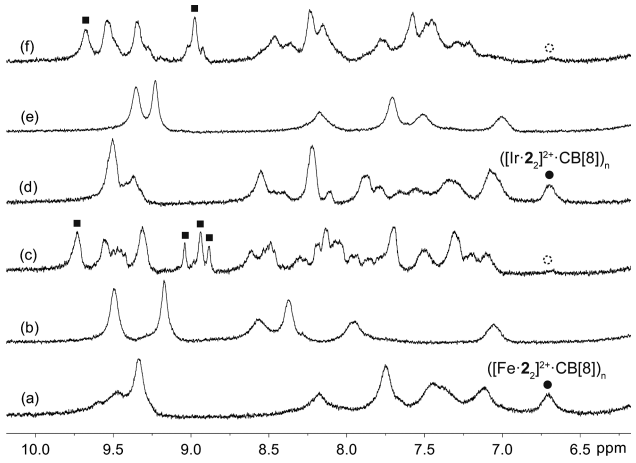

Figure 8. ^{1}H NMR spectra of (a) homo-oligomer $([Fe{\cdot}\mathbf{2}_2]^{2+}{\cdot}CB[8])_n$, (b) homo-oligomer $([Ir{\cdot}\mathbf{3}_2]^{3+}{\cdot}CB[8])_n$, (c) hetero-oligomer $([Fe{\cdot}\mathbf{2}_2]^{2+}{\cdot}CB[8]{\cdot}[Ir{\cdot}\mathbf{3}_2]^{3+}{\cdot}CB[8])_n$, (d) homo-oligomer $([Ir{\cdot}\mathbf{2}_2]^{3+}{\cdot}CB[8])_n$, (e) homo-oligomer $([Fe{\cdot}\mathbf{3}_2]^{2+}{\cdot}CB[8])_n$, and (f) hetero-oligomer $([Ir{\cdot}\mathbf{2}_2]^{3+}{\cdot}CB[8]{\cdot}[Fe{\cdot}\mathbf{3}_2]^{2+}{\cdot}CB[8])_n$. Black dots and dashed circles highlight the disappearance of the signature signal for naphthyl/naphthyl interactions, and black squares highlight the formation of new characteristic signals of the hetero-oligomers.

stoichiometric amounts of CB[8], which acts as a "soft", noncovalent connector between metal/terpyridine complexes.

■ ASSOCIATED CONTENT

Supporting Information

Preparation and characterization of ligands **1**–**3**, as well as their Fe(II) and Ir(III) complexes; titration of metal–ligand complexes with CB[7] and CB[8]; ITC results; DOSY calibration; distance measurements by 2D NOESY experiments; Cartesian coordinates of the optimized structure of assemblies $[Ir{\cdot}\mathbf{1}_2]^{3+}{\cdot}(CB[7])_2$ and $([Fe{\cdot}\mathbf{2}_2]^{2+})_2{\cdot}CB[8]$. This material is available free of charge via the Internet at http://pubs.acs.org.

■ AUTHOR INFORMATION

Corresponding Author

masson@ohio.edu

Notes

The authors declare no competing financial interest.

■ ACKNOWLEDGMENTS

This work was supported by the American Chemical Society Petroleum Research Fund (PRF No. 51053–ND4), the Department of Chemistry and Biochemistry, the College of Arts and Sciences and the Vice President for Research at Ohio University. We thank the Ohio Supercomputer Center (OSC) in Columbus for its generous allocation of computing time.

■ REFERENCES

(1) (a) Mock, W. L.; Shih, N. Y. *J. Org. Chem.* **1986**, *51*, 4440–4446. For two reviews covering the recognition properties and applications of CB[n] (n = 5– 8, 10), see: (b) Lagona, J.; Mukhopadhyay, P.; Chakrabarti, S.; Isaacs, L. *Angew. Chem., Int. Ed.* **2005**, *44*, 4844–4870. (c) Masson, E.; Ling, X.; Joseph, R.; Kyeremeh-Mensah, L.; Lu, X. *RSC Adv.* **2012**, *2*, 1213–1247.

(2) (a) Rekharsky, M. V.; Mori, T.; Yang, C.; Ko, Y. H.; Selvapalam, N.; Kim, H.; Sobransingh, D.; Kaifer, A. E.; Liu, S.; Isaacs, L.; Chen, W.; Moghaddam, S.; Gilson, M. K.; Kim, K.; Inoue, Y. *Proc. Natl. Acad. Sci. U. S. A.* **2007**, *104*, 20737–20742. (b) Moghaddam, S.; Yang, C.;

Rekharsky, M.; Ko, Y. H.; Kim, K.; Inoue, Y.; Gilson, M. K. *J. Am. Chem. Soc.* **2011**, *133*, 3570−3581. (c) Ko, Y. H.; Hwang, I.; Lee, D. W.; Kim, K. *Isr. J. Chem.* **2011**, *51*, 506−14.

(3) (a) Florea, M.; Nau, W. M. *Angew. Chem., Int. Ed.* **2011**, *50*, 9338−9342. (b) Biedermann, F.; Uzunova, V. D.; Scherman, O. A.; Nau, W. M.; Simone, A. D. *J. Am. Chem. Soc.* **2012**, *134*, 15318−15323. (c) Nau, W. M.; Florea, M.; Assaf, K. I. *Isr. J. Chem.* **2011**, *51*, 559−577. (d) Marquez, C.; Nau, W. M. *Angew. Chem., Int. Ed.* **2001**, *40*, 4387−4390. (e) Mohanty, J.; Nau, W. M. *Angew. Chem., Int. Ed.* **2005**, *44*, 3750−3754. (f) Koner, A. L.; Nau, W. M. *Supramol. Chem.* **2007**, *19*, 55−66.

(4) (a) Grimme, S.; Ehrlich, S.; Goerigk, L. *J. Comput. Chem.* **2011**, *32*, 1456−1465. (b) Grimme, S. *Chem.—Eur. J.* **2012**, *18*, 9955−9964.

(5) (a) Gerasko, O. A.; Samsonenko, D. G.; Fedin, V. P. *Russ. Chem. Rev.* **2002**, *71*, 741−760. (b) Whang, D.; Heo, J.; Park, J. H.; Kim, K. *Angew. Chem., Int. Ed.* **1998**, *37*, 78−80. (c) Jeon, Y. M.; Kim, J.; Whang, D.; Kim, K. *J. Am. Chem. Soc.* **1996**, *118*, 9790−9791. (d) Abramov, P. A.; Adonin, S. A.; Peresypkina, E. V.; Sokolov, M. N.; Fedin, V. P. *J. Struct. Chem.* **2010**, *51*, 731−736.

(6) (a) Gerasko, O. A.; Sokolov, M. N.; Fedin, V. P. *Pure Appl. Chem.* **2004**, *76*, 1633−1646. (b) Samsonenko, D. G.; Sokolov, M. N.; Virovets, A. V.; Pervukhina, N. V.; Fedin, V. P. *Eur. J. Inorg. Chem.* **2001**, 167−172. (c) Algarra, A. G.; Sokolov, M. N.; González-Platas, J.; Fernández-Trujillo, M. J.; Basallote, M. G.; Hernández-Molina, R. *Inorg. Chem.* **2009**, *48*, 3639−3649. (d) Bernal, I.; Mukhopadhyay, U.; Virovets, A. V.; Fedin, V. P.; Clegg, W. *Chem. Commun.* **2005**, 3791−3792.

(7) (a) Collin, J. P.; Dixon, I. M.; Sauvage, J. P.; Williams, J. A. G.; Barigelletti, F.; Flamigni, L. *J. Am. Chem. Soc.* **1999**, *121*, 5009−5016. (b) Flamigni, L.; Collin, J. P.; Sauvage, J. P. *Acc. Chem. Res.* **2008**, *41*, 857−871. (c) Tang, B.; Yu, F.; Li, P.; Tong, L.; Duan, X.; Xie, T.; Wang, X. *J. Am. Chem. Soc.* **2009**, *131*, 3016−3023. (d) Wild, A.; Winter, A.; Hager, M. D.; Görls, H.; Schubert, U. S. *Macromol. Rapid Commun.* **2012**, *33*, 517−521. (e) Newkome, G. R.; Cho, T. J.; Moorefield, C. N.; Mohapatra, P. P.; Godínez, L. A. *Chem.—Eur. J.* **2004**, *10*, 1493−1500.

(8) (a) Kar, T.; Scheiner, S. *J. Phys. Chem. A* **2004**, *108*, 9161−9168. (b) Scheiner, S.; Kar, T. *J. Phys. Chem. A* **2008**, *112*, 11854−11860.

(9) (a) Baleja, J. D.; Moult, J.; Sykes, B. D. *J. Magn. Reson.* **1990**, *87*, 375−384. (b) Mugridge, J. S.; Zahl, A.; van Eldik, R.; Bergman, R. G.; Raymond, K. N. *J. Am. Chem. Soc.* **2013**, *135*, 4299−4306.

(10) (a) Tao, J.; Perdew, J. P.; Staroverov, V. N.; Scuseria, G. E. *Phys. Rev. Lett.* **2003**, *91*, 146401−146404. (b) Grimme, S.; Antony, J.; Ehrlich, S.; Krieg, H. *J. Chem. Phys.* **2010**, *132*, 154104−154119.

(11) (a) Klamt, A.; Schüürmann, G. *J. Chem. Soc. Perkin Trans. 2* **1993**, *5*, 799−805. (b) Klamt, A.; Jonas, V. *J. Chem. Phys.* **1996**, *105*, 9972−9980. The COSMO model uses a hypothetical solvent of infinite relative permittivity; the error caused by this approximation is insignificant for highly polar solvents like water.

(12) (a) Bühl, M.; Reimann, C.; Pantazis, D. A.; Bredow, T.; Neese, F. *J. Chem. Theory Comput.* **2008**, *4*, 1449−1459. (b) Vícha, J.; Patzschke, M.; Marek, R. *Phys. Chem. Chem. Phys.* **2013**, *15*, 7740−7754.

(13) (a) McDonald, I. K.; Thornton, J. M. *J. Mol. Biol.* **1994**, *238*, 777−793. (b) Arunan, E.; Desiraju, G. R.; Klein, R. A.; Sadlej, J.; Scheiner, S.; Alkorta, I.; Clary, D. C.; Crabtree, R. H.; Dannenberg, J. J.; Hobza, P.; Kjaergaard, H. G.; Legon, A. C.; Mennucci, B.; Nesbitt, D. J. *Pure Appl. Chem.* **2011**, *83*, 1637−1641.

(14) Rekharsky, M. V.; Yamamura, H.; Kawai, M.; Osaka, I.; Arakawa, R.; Sato, A.; Ko, Y. H.; Selvapalam, N.; Kim, K.; Inoue, Y. *Org. Lett.* **2006**, *8*, 815−818.

(15) Marcus, Y. *Biophys. Chem.* **1994**, *51*, 111−127.

(16) See (a) Gupta, S.; Choudhury, R.; Krois, D.; Brinker, U. H.; Ramamurthy, V. *J. Org. Chem.* **2012**, *77*, 5155−5160. (b) Choudhury, R.; Gupta, S.; Da Silva, J. P.; Ramamurthy, V. *J. Org. Chem.* **2013**, *78*, 1824−1832. (c) Yu, J. S.; Wu, F. G.; Tao, L. F.; Luo, J. J.; Yu, Z. W. *Phys. Chem. Chem. Phys.* **2011**, *13*, 3638−3641. (d) Lee, S. J. C.; Lee, J. W.; Lee, H. H.; Seo, J.; Noh, D. H.; Ko, Y. H.; Kim, K.; Kim, H. I. *J. Phys. Chem. B* **2013**, *117*, 8855−8864. (e) Joseph, R.; Masson, E. *Org. Biomol. Chem.* **2013**, *11*, 3116−3127. (f) Yu, J. S.; Wu, F. G.; Zhou, Y.; Zheng, Y. Z.; Yu, Z. W. *Phys. Chem. Chem. Phys.* **2012**, *14*, 8506−8510 as well as ref 1c for the exhaustive list of all references that have contributed to this plot.

(17) For an excellent review that describes the use of parameters for hydrogen bonding to predict host−guest recognition patterns, see: Hunter, C. A. *Angew. Chem., Int. Ed.* **2004**, *43*, 5310−5324.

(18) (a) Fang, R.; Liu, Y.; Wang, Z.; Zhang, X. *Polym. Chem.* **2013**, *4*, 900−903. (b) Liu, Y.; Fang, R.; Tan, X.; Wang, Z.; Zhang, X. *Chem.—Eur. J.* **2012**, *18*, 15650−15654. (c) Liu, Y.; Yang, H.; Wang, Z.; Zhang, X. *Chem.—Asian J.* **2013**, *8*, 1626−1632. (d) Liu, Y.; Huang, Z.; Tan, X.; Wang, Z.; Zhang, X. *Chem. Commun.* **2013**, *49*, 5766−5768.

(19) It is 0.33 in the case of spherical species (based on the Stokes−Einstein equation) and a linear correlation between volumes and molecular weights; 0.50 according to the Zimm model; see Shimada, K.; Kato, H.; Saito, T.; Matsuyama, S.; Kinugasa, S. *J. Chem. Phys.* **2005**, *122*, 244914−244920 for details.

(20) Subscript "*n*" is used indiscriminately throughout the study, although the length of each oligomer varies depending on its composition.

(21) (a) Patrick, C. R.; Prosser, G. S. *Nature* **1960**, *187*, 1021. (b) Williams, J. H. *Acc. Chem. Res.* **1993**, *26*, 593−598. (c) Tsuzuki, S.; Uchimaru, T.; Mikami, M. *J. Phys. Chem. A* **2006**, *110*, 2027−2033.